Supporting Information for

Depressing Irreversible Reaction on Three-Dimensional Interface towards High Areal Capacity Lithium Metal Anode

Wei Deng[†, a], Shanshan Liang[†, a, b], Xufeng Zhou[, a], Fei Zhao[a], Wenhua Zhu[a], and Zhaoping Liu[*, a]*

Dr. W. Deng, Miss. S. Liang, Prof. Dr. X. Zhou, Mr. F. Zhao, Mr. W. Zhu, Prof. Dr. Z. Liu

a Key Laboratory of Graphene Technologies and Applications of Zhejiang Province and Advanced Li-ion Battery Engineering Laboratory of Zhejiang Province, Ningbo Institute of Materials Technology & Engineering, Chinese Academy of Sciences, Zhejiang 315201, P. R. China

b Department of Polymer Materials, Shanghai University, Shanghai 200444, P. R. China

† These authors contribute equally to this work.

* Corresponding authors. Tel./Fax: +86-574-8668-5096.

E-mail address: zhouxf@nimte.ac.cn, liuzp@nimte.ac.cn.

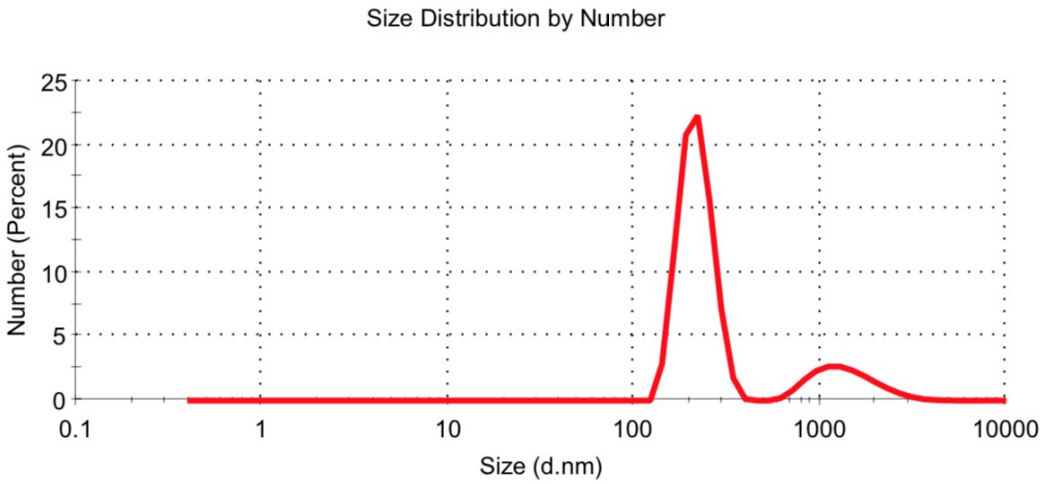

Figure S1. Size distribution of GO sheets dispersed in water.

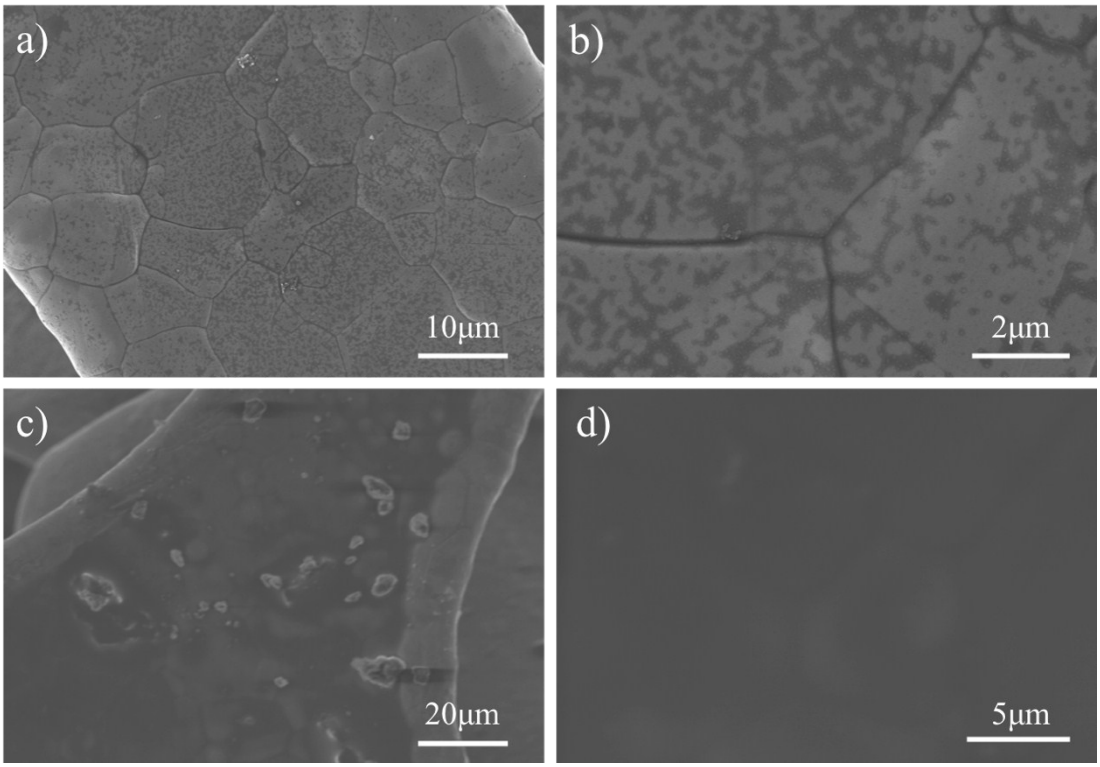

Figure S2. SEM images of SPE coated Ni foam with different volumes of coating solutions of 100 μL (a, b) and 400 μL (c, d).

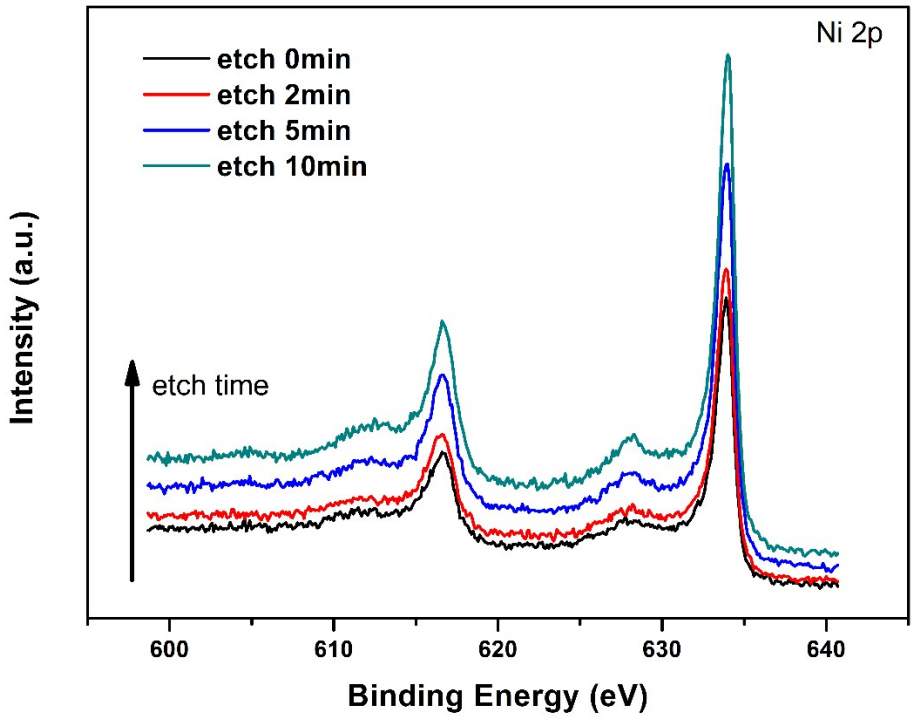

Figure S3. Ni 2p XPS spectra of Ni foam/uSPE after etching with different time.

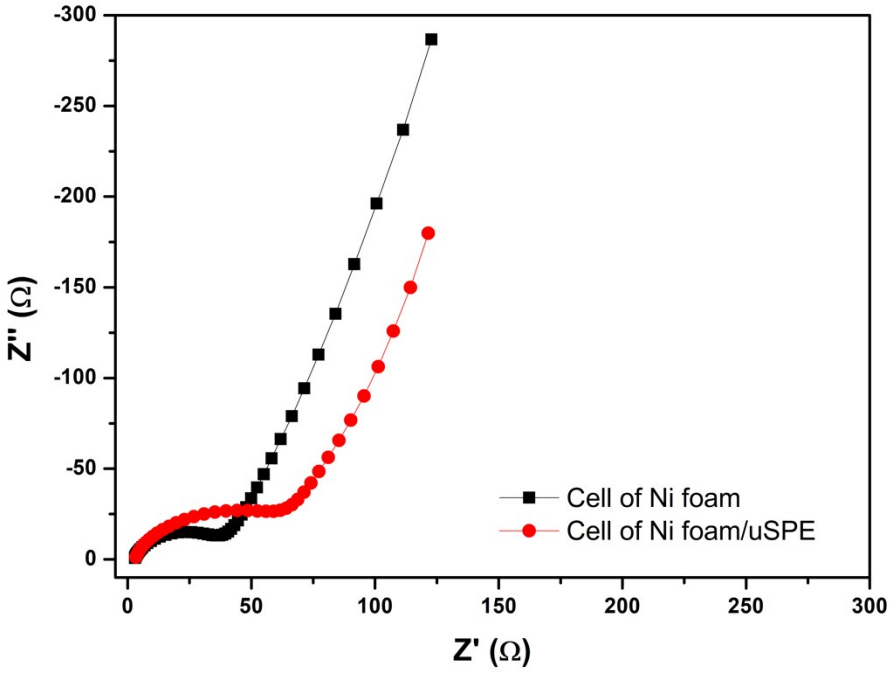

Figure S4. EIS profiles of fresh cells of Ni foam and Ni foam/uSPE when paired with Li foil.

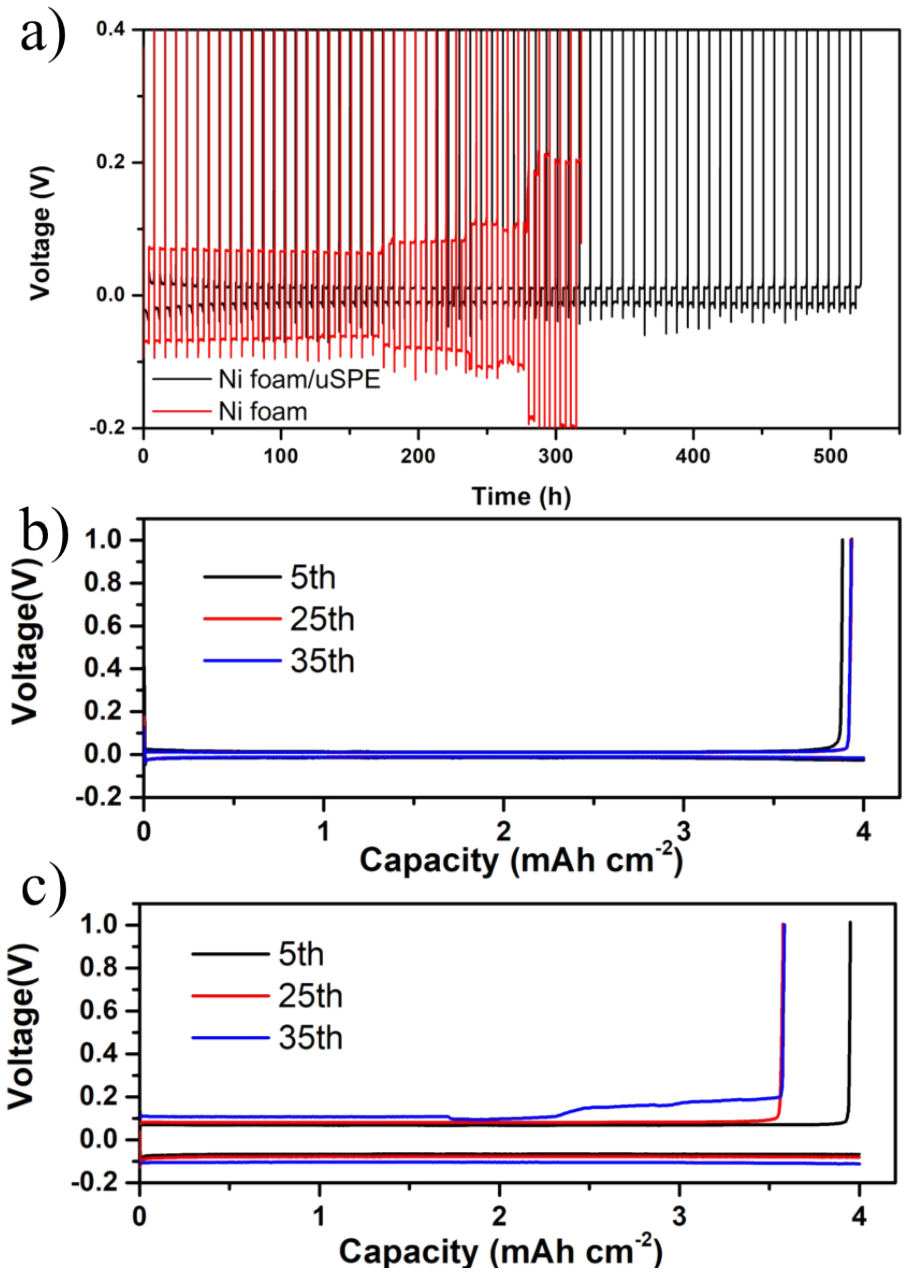

Figure S5. (a) Voltage profiles of Ni foam and Ni foam/uSPE under areal capacity of 4.0 mAh cm^{-2} and current density of 1.0 mA cm^{-2}. Their corresponding charge/discharge profiles at specific cycles of Ni foam/uSPE (b) and Ni foam (c).

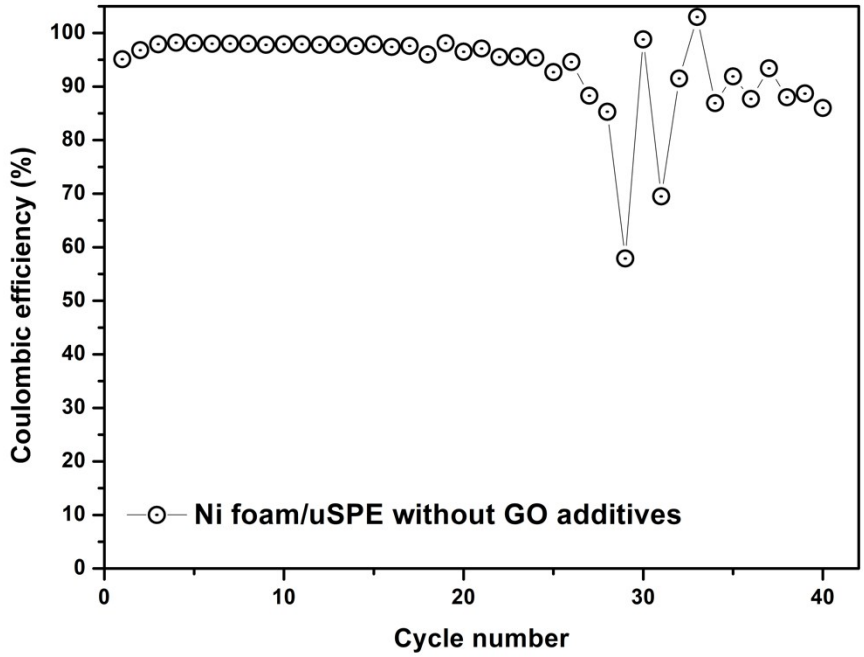

Figure S6. CE performance of Ni foam/uSPE without GO additives under current density of 1.0 mA cm^{-2} and areal capacity of 10.0 mAh cm^{-2}.

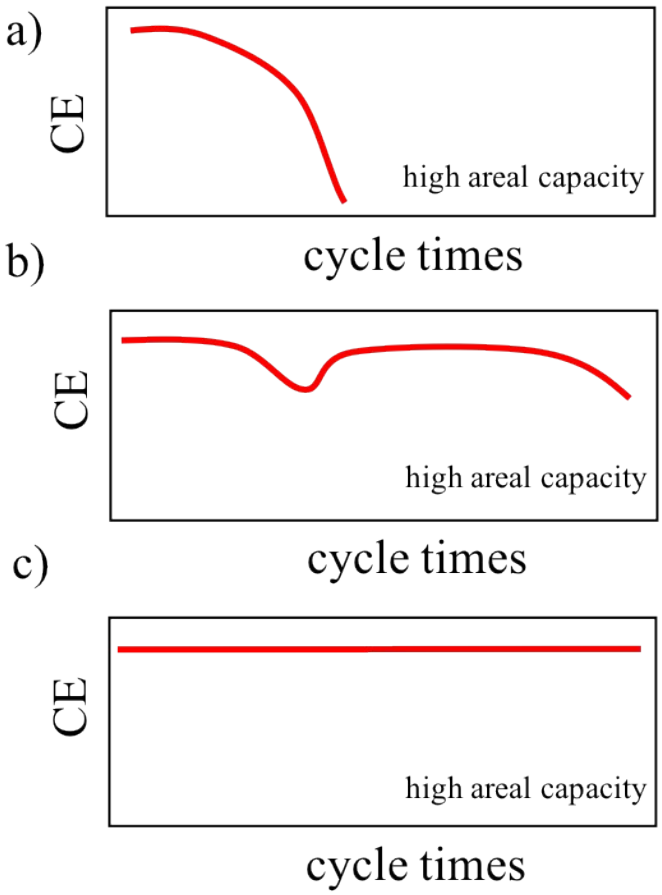

Figure S7. Simplified characteristic CE variation profile of metal foil (a), metal foam (b) and uSPE coated metal foam (c) along with cycle time according to experimental results in this work and in previous reports.

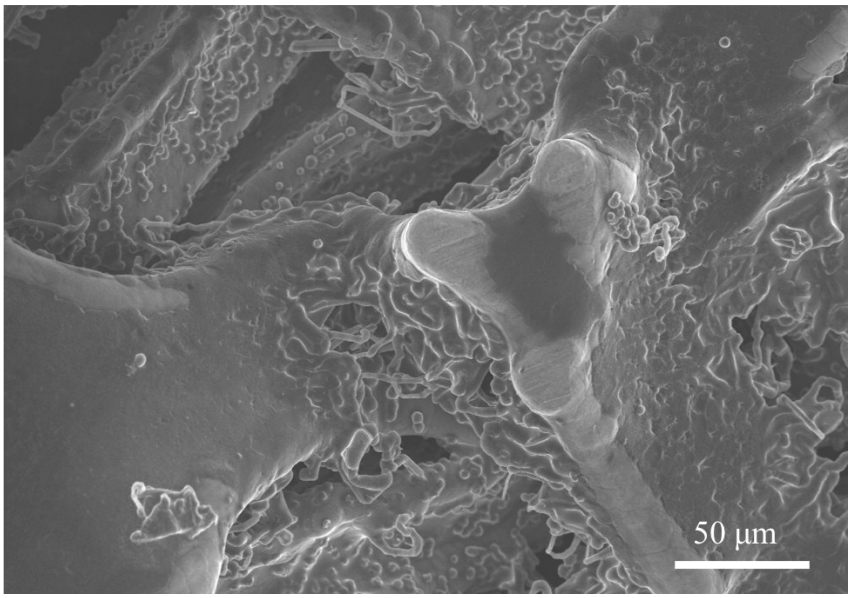

Figure S8. Surface morphology of Ni foam after 10 cycles of stripping/plating under areal capacity of 10.0 mA h cm^{-2}.

Table S1. Comparison of current density, areal capacity and CE of Li metal anode in this work with those in previous researches.

Reference	Sample Name	Current density	Areal capacity	Coulombic efficiency
S[1]	Nanochannel Cu	1 mA cm^{-2}	0.5 mAh cm^{-2}	97.6%
S[2]	graphite C fiber	1 mA cm^{-2}	8 mAh cm^{-2}	98.0%
S[3]	porous Cu	0.5 mA cm^{-2}	0.5 mAh cm^{-2}	98.6%
S[4]	hollow C fiber	1 mA cm^{-2}	6 mAh cm^{-2}	99.0%
S[5]	3D Cu	1 mA cm^{-2}	5 mAh cm^{-2}	96.0%
S[6]	Au/rGO	0.5 mA cm^{-2}	5 mAh cm^{-2}	98.0%
S[7]	CuNWs@GE	1 mA cm^{-2}	2 mAh cm^{-2}	97.0%
S[8]	Cu nanowire	1 mA cm^{-2}	5 mAh cm^{-2}	98.6%
S[9]	VA-Cu	1 mA cm^{-2}	3 mAh cm^{-2}	98.5%
S[10]	porous Cu	1 mA cm^{-2}	1 mAh cm^{-2}	97.0%
S[11]	CFC/G/ZnO	1 mA cm^{-2}	12 mAh cm^{-2}	98.0%
This work	**Ni foam/uSPE**	**1 mA cm^{-2}**	**10 mAh cm^{-2}**	**98.9%**

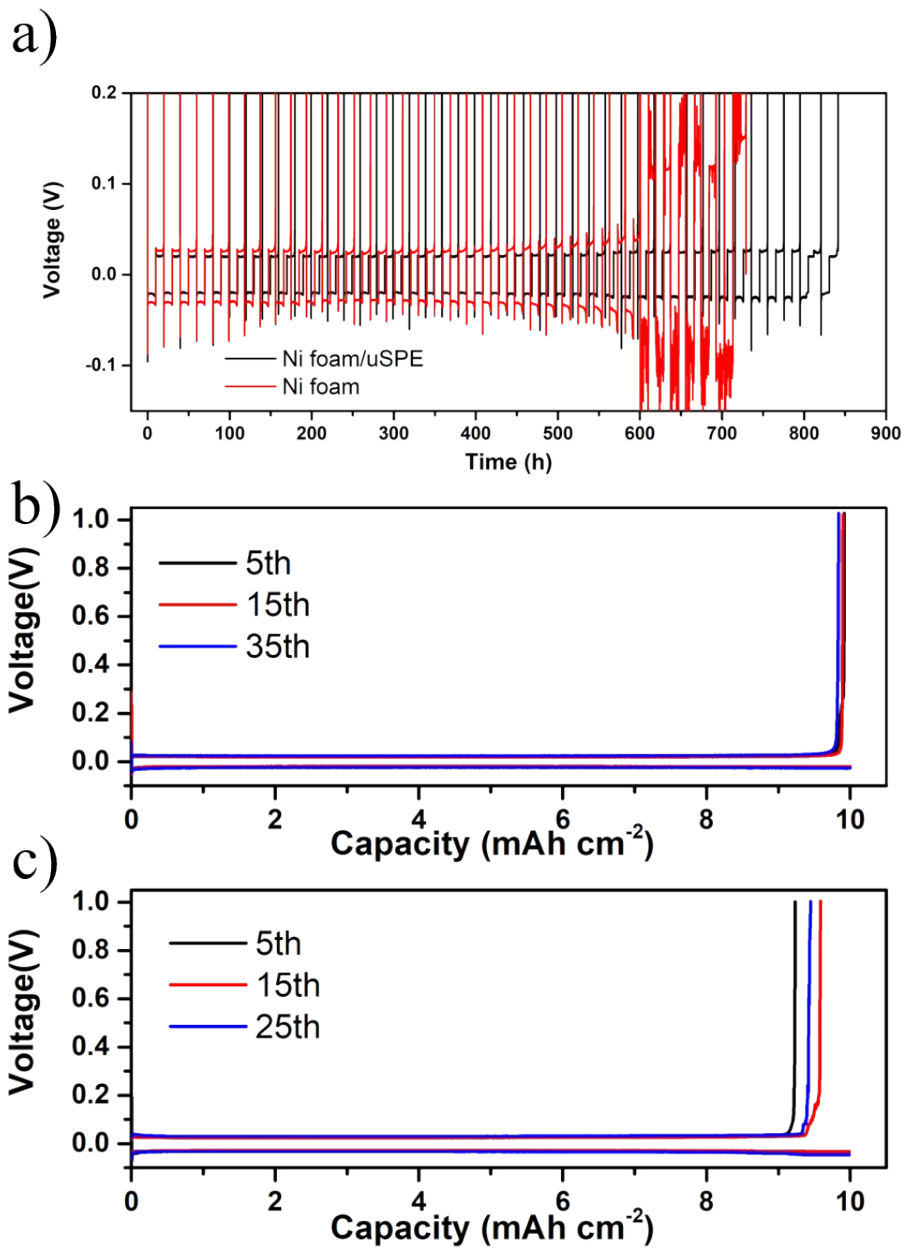

Figure S9. (a) Voltage profiles of Ni foam and Ni foam/uSPE under areal capacity of 10.0 mAh cm^{-2} and current density of 1.0 mA cm^{-2}. Their corresponding charge/discharge profiles at specific cycles of Ni foam/uSPE (b) and Ni foam (c).

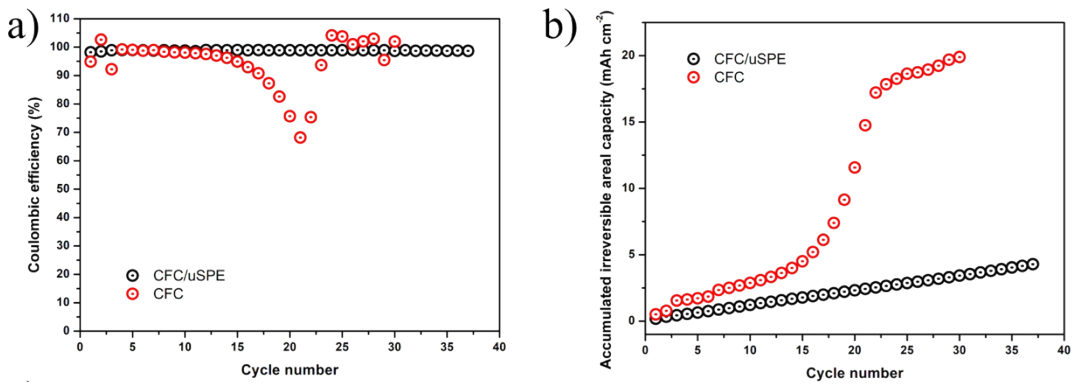

Figure S10. CE performance (a) and accumulated irreversible areal capacities (b) of CFC and CFC/uSPE at areal capacity of 10.0 mAh cm^{-2} under current density of 1.0 mA cm^{-2}.

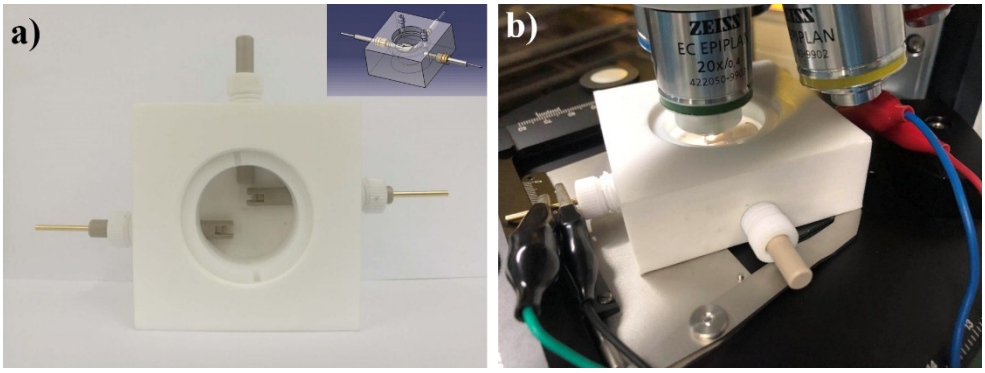

Figure S11. (a) The optical image for operando cell and insets in (a) is its design model. (b) The image shows how the operando cell is linked with a microscope.

Reference:

[1] W. Liu, D. C. Lin, A. Pei, Y. Cui, Journal of the American Chemical Society 2016, 138, 15443.

[2] T. T. Zuo, X. W. Wu, C. P. Yang, Y. X. Yin, H. Ye, N. W. Li, Y. G. Guo, Advanced Materials 2017, 29, 1700389.

[3] C. P. Yang, Y. X. Yin, S. F. Zhang, N. W. Li, Y. G. Guo, Nat Commun 2015, 6, 8058.

[4] L. Liu, Y.-X. Yin, J.-Y. Li, N.-W. Li, X.-X. Zeng, H. Ye, Y.-G. Guo, L.-J. Wan,

Joule 2017, 1, 563.

[5] F. Shen, F. Zhang, Y. Zheng, Z. Fan, Z. Li, Z. Sun, Y. Xuan, B. Zhao, Z. Lin, X. Gui, X. Han, Y. Cheng, C. Niu, Energy Storage Materials 2018, 13, 323.

[6] J. Pu, J. C. Li, Z. H. Shen, C. L. Zhong, J. Y. Liu, H. X. Ma, J. Zhu, H. G. Zhang, P. V. Braun, Advanced Functional Materials 2018, 28, 1804133.

[7] K. Yan, B. Sun, P. Munroe, G. Wang, Energy Storage Materials 2018, 11, 127.

[8] L.-L. Lu, J. Ge, J.-N. Yang, S.-M. Chen, H.-B. Yao, F. Zhou, S.-H. Yu, Nano Letters 2016, 16, 4431.

[9] S. H. Wang, Y. X. Yin, T. T. Zuo, W. Dong, J. Y. Li, J. L. Shi, C. H. Zhang, N. W. Li, C. J. Li, Y. G. Guo, Adv Mater 2017, 29, 1703729.

[10] Q. Yun, Y. B. He, W. Lv, Y. Zhao, B. Li, F. Kang, Q. H. Yang, Adv Mater 2016, 28, 6932.

[11] W. Deng, W. Zhu, X. Zhou, Z. Liu, Energy Storage Materials 2018, 15, 266.